Design of a Unit Cell Facility for Studies of the Prismatic VHTR Lower Plenum

D. Tyler Landfried, Paul Kristo
University of Pittsburgh
3700 O'Hara St, Pittsburgh, PA 15213, USA
dtl5@pitt.edu , pjk26@pitt.edu

Mark Kimber
Associate Professor, Department of Mechanical Engineering and Material Science
University of Pittsburgh
3700 O'Hara St, Pittsburgh, PA 15213, USA
mlk53@pitt.edu

ABSTRACT

One proposed design for a Generation IV reactor is the very high temperature gas reactor, which uses helium as the primary coolant due to its advantageous properties as an inert gas. One area of concern for the VHTR is the lower plenum, where temperature differences as high as 300-400 K can cause hot streaking. The lower plenum consists of a series of structural posts and an array of coolant jets which lead to a singular outlet from the reactor core. The objective of this study is to present the design for an experimental facility where insight can be gained into flow physics within the VHTR lower plenum. To study the lower plenum mixing behavior, an experimental setup including a test section herein called the 'unit cell' is designed. The unit cell consists of six hexagonally arranged jets directing their flow into the test section and subsequently traveling through a hexagonal array of seven support posts, all in the presence of a cross flow. Temperature profiles are captured via multiple thermocouples embedded in each post. With the 6 jets whose outlets are on the top face of the test section, along with the cross flow at the inlet of the test section, the unit cell is capable of experimentally simulating notable post and jet configurations found in the lower plenum. With the radial temperature profiles, the thermal fluctuations and flow behavior on these posts can be studied. The present work focuses on the scaling and design of the unit cell facility. This facility will be used to provide high quality experimental data for future validation studies as well aid to achieve more comprehensive understanding of the loading conditions which cause the thermal stresses experienced by the structural support posts in the lower plenum of the VHTR.

KEYWORDS
Unit Cell, Very High Temperature Reactor, Impinging Jets, Bank of Cylinders

1. INTRODUCTION

The Very High Temperature Reactor (VHTR) is a next generation nuclear reactor, one of the six concepts originally proposed by the Generation IV International Forum. The VHTR incorporates Helium as the coolant to extract heat from the core, and subsequently is used for high-efficiency production of either electricity or hydrogen. Contrary to modern Light Water Reactors (LWRs) which have water flow upward through the reactor, the Helium coolant travels vertically downward through the VHTR core extracting heat from the core before discharging into the lower plenum much like an impinging array of jets. Due to the non-uniform heat generation in the core and flow maldistribution, the temperature and velocity of these jets

directed into the lower plenum can vary significantly. Once in the lower plenum, the flow of these jets changes directions 90° and traverses across a staggered array of cylindrical posts. Current designs for the VHTR lower plenum 272 jets issuing into a staggered array of 196 posts. In this design, there are 68 83.8 mm jets, 72 116.8 mm jets, and 132 144.8 mm jets which can vary in both inlet temperature and mass flow rate. The temperature of these jets can vary from 1049.6 K to 1371.4 K with velocities ranging from 12.08 m/s to 148.7 m/s [1, 2]. From preliminary simulations of a symmetric half-model of the lower plenum conducted by Mazumdar et al. [2], it is observed there are thermal "hot streaks" that interact with neighboring cold streaks in close proximity to posts and other important structures in the flow, as shown in Figure 1. These hot streaks in conjunction with diverse velocity gradients, as shown in Figure 2 which is generated from data presented in Mazumdar et al. [2]. As shown in Figure 2 the velocity is the lower plenum is normally less than the average velocity at the outlet, 70 m/s.

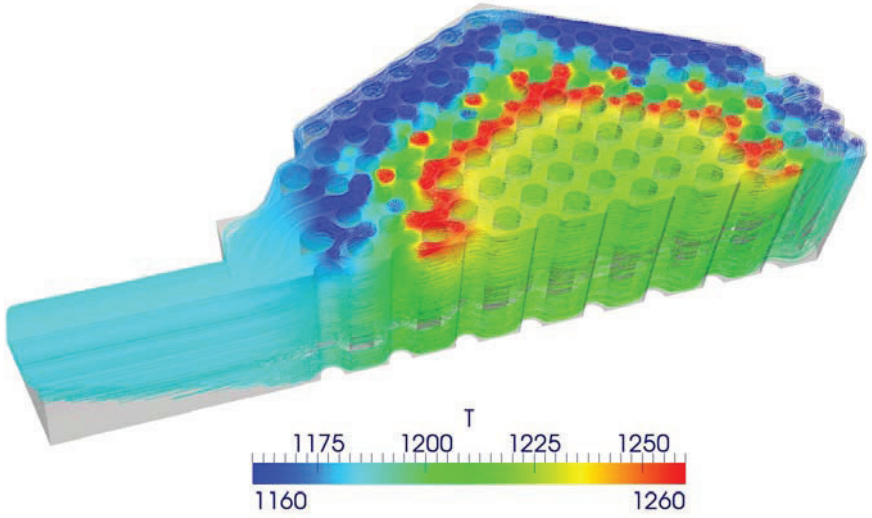

Figure 1: CFD prediction of streamlines colored with temperature [K] in the lower plenum of a VHTR [2].

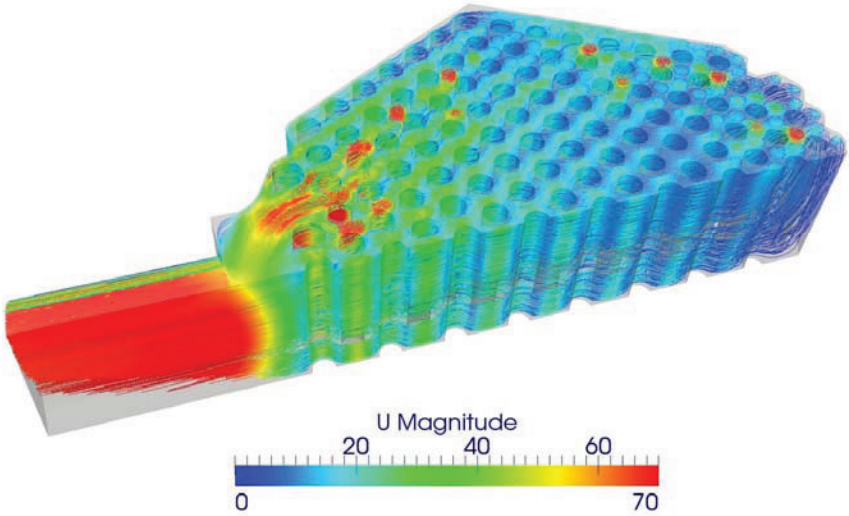

Figure 2: CFD prediction of streamlines colored with velocity magnitude [m/s] in the lower plenum of a VHTR (Magnitudes greater than 70 m/s appear red). Adapted from data in [2].

The hot streaks shown in Figure 1, caused by the non-isothermal mixing, raise major concerns regarding structural failure due to thermal fatigue, since temperature fluctuations in fluid flow can ultimately be transmitted to the support structure. This phenomenon is known as thermal striping, and represents a significant challenge for the next generation gas cooled nuclear reactors. The complicated velocity field and highly stratified temperature field make thermal striping in the lower plenum complicated to study. Due to limitations in experimental setups, related to the high temperature and velocities expected in the lower plenum, there has been interest in numerical modeling of the lower plenum flows. However to properly utilize numerical modeling verification and validation of the models is necessary to understand their capabilities and limitations in the complex flows expected. In order to elucidate the present physics, work by Condie et al. [3] identified several canonical problems where validation and verification of numerical models is necessary, including a single jet in confined crossflow and multiple jet arrays in both confined and unconfined flow across tube bundles.

In order to provide validation and verification of the numerical models a new problems, referred to as the unit cell, is proposed. The unit cell consists of a hexagonal impinging jet array issuing parallel to a tube bundle experiencing a crossflow. Following is a description of previous scaled studies related to the VHTR, analysis of scaling in the lower plenum, and design of the unit cell experiment.

2. BACKGROUND

Several previous studies have looked at simplified models of the complex flow present in the VHTR. Investigators at the Idaho National Laboratory (INL) have performed numerous experimental isothermal studies, utilizing a matched index of refraction (MIR) setup, which are aimed at characterizing the turbulence in the VHTR lower plenum [4-11]. The INL facility, shown in Figure 3, is a 6.55:1 scale model of a portion of the lower plenum used only with isothermal flows. Accordingly, the MIR facility was a water and mineral oil mixture based experiment capable of producing jet Reynolds numbers as large as approximately 1280 with cross flow Reynolds numbers, based on the slot width, of about 3300 [3].

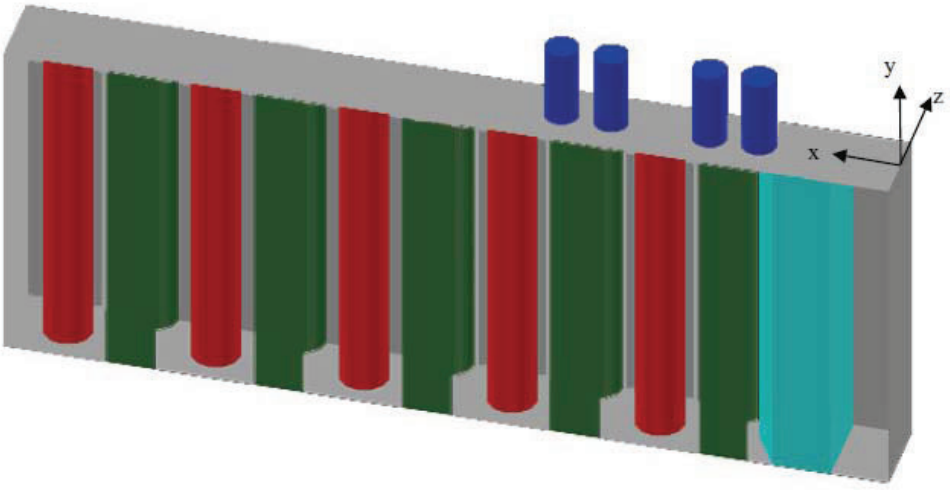

Figure 3: INL's MIR facility [3]
Green/red posts, blue jets, turquoise crossflow inlet

Measurements on the same geometry used by INL (Figure 3) Smith et al. [12] investigated isothermal velocity and pressure measurements for flow across a confined row of cylinders using PIV measurements in air for post Reynolds numbers up varying from the laminar range to the fully turbulent range (1,000-

55,000). Careful concern was given to quantifying spanwise profiles of the Reynolds stresses as well as wake length and recirculation length downstream of each cylinder. Additional isothermal experimental studies of the lower plenum have been carried out by Amini and Hassan [13], who studied jets issuing perpendicularly into a tube bundle. Utilizing full field PIV mean and fluctuating velocity components as well as Reynolds Stresses were determined for jet Reynolds numbers of 4,500 and 13,400 at different heights along the tube bundles.

Continuing on the experimental results of Smith et al. [12], further investigation into validation of numerical simulations was conducted [14]. A k-ω unsteady Reynolds average Navier-Stokes (uRANS) model and two detached eddy simulations (DES) compared both global and local phenomena in the flow domain.

Further work has looked at full field simulations of the lower plenum, but currently there is not any validation data available for the simulations. Rodriguez and El-Genk [15] performed numerical simulations of a half model of lower plenum using a very coarse grid Large Eddy Simulation (LES) with helium as the working fluid. Specific attention was given to determining the mixing and spreading of each single hot jet as its momentum is swept away by a cooler cross flow produced by the other jets. Different magnitudes of swirl were investigated and it was observed that the presence of swirl increased thermal mixing and reduced hot streaking.

3. SCALING AND THE UNIT CELL MODEL

Before examining the three unit cell cases detailed in Figure 4, the extensive VHTR lower plenum scaling studies conducted by INL [9-11] were reviewed. As explained by Condie et al. [3] based on expected Richardson numbers it is reasonable to assume that during full power operation the jets in the lower plenum are momentum-driven with negligible buoyancy effects. Based on the preliminary simulations conducted by Mazumdar et al [2], scaling of the lower plenum was investigated. In lower plenum the jet Reynolds numbers vary from 10^3 to 10^5, while the transverse Reynolds number, calculated based on the cross flow velocity and jet diameter, be as large as 51,000 assuming a maximum crossflow velocity of 70 m/s. In areas with large transverse velocities (~50 m/s) the transverse velocity ratio ($R = V_{jet}/V_{trans}$) can be less than one half. For locations with minimal transverse flow near the edges of the plenum, transverse velocity ratio can be very large (~70 based on a maximum jet velocity of 148 m/s [2]) as the transverse velocity approaches zero. However typical of the majority of the jets in the lower plenum is a transverse velocity ratio between 0.5-5. Similarly, in the lower plenum post Reynolds numbers reach 70,000 with shedding frequencies of approximately 60 Hz.

In order to expand upon current studies related to isothermal and non-isothermal flows in the lower plenum, an experimental facility is designed to enable high quality data collection for future validation studies. The complex lower plenum flow is actually comprised of multiple canonical flow features including flow across tube bundles, impinging jet arrays, and jets in cross flow, also known as transverse jets. A repeating flow configuration, referred to as the unit cell is the focus of this experimental facility, and consists of six jets arranged in a hexagonal pattern whose flow enters the test section with the dominant flow direction along the length of the seven cylindrical support posts. This flow is then met by an orthogonal crossflow. Shown in Figure 4 is a half model of the VHTR lower plenum with three unique configurations of this unit cell geometry, labeled Case A, B, and C. By adjusting the velocities and temperatures of the six jets and the strength and temperature of the crossflow, different regions of the lower plenum can be experimentally simulated. Each of the cases have unique flow features that are considered during the design. Design of the facility is achieved using standard scaling requirements for matching many non-dimensional parameters in the VHTR lower plenum including jet Reynolds number, post Reynolds number and vortex shedding frequency, transverse Reynolds number, and plenum Reynolds number, as well as maintaining geometric similarity.

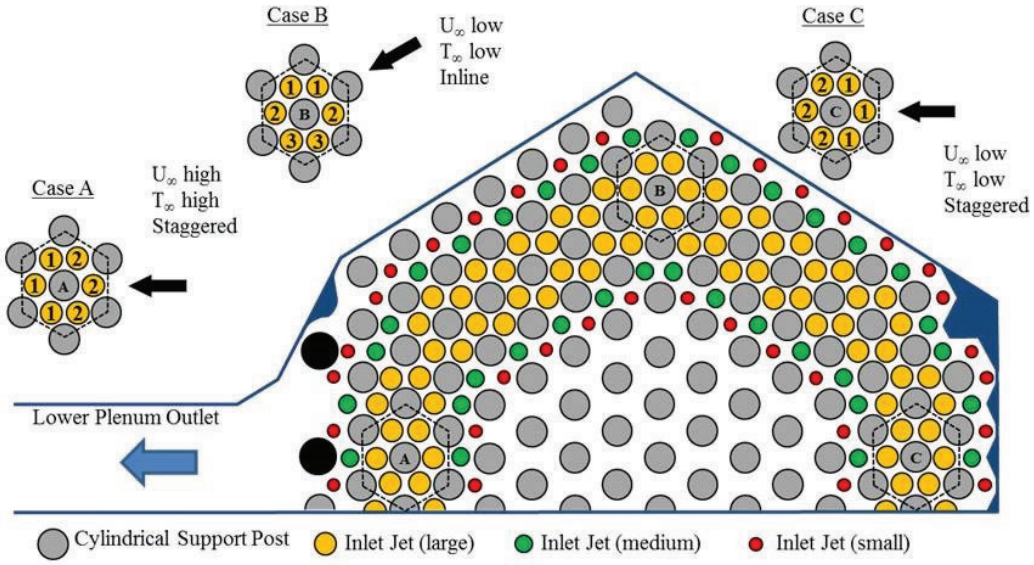

Figure 4: Half Model of VHTR Lower Plenum with Three Proposed Unit Cell Test Cases

The unit cell experimental facility is designed to work in conjunction with an existing flow motivation skid detailed in [16]. The previously designed flow skid is capable of creating three simultaneous flows at different temperatures and flowrates. The channel flow rates, measured via pressure drop across a high accuracy orifice flow plate and controlled via a PID logic automated valve, can be varied up to 6.96 L/s (14.75 cfm) which for a 22.225 mm (0.875in) jet corresponds to a jet Reynolds number of 24,600. The uncertainty in flow rate is 2.5% (0.08 cfm) for jet a Reynolds number of 5,000 but decreases to 0.27% (0.04 cfm) for the maximum jet Reynolds number. Each channel has independent PID controlled heaters capable of producing jet temperatures in excess of 410 K. The jet temperatures have an accuracy of ± 0.4 K.

For the unit cell experimental facility, shown in Figure 4, three unique flow patterns typical of what is experienced in the lower plenum have been identified. The first, labeled Case A, involves two different temperature jets entering the lower plenum with a strong cross flow induced by the others jets which mix and flow past the unit cell similar to flow past a staggered tube bundle. In this region the maximum velocity ratio $R = V_{jet}/V_{trans}$, where V_{jet} is the jet velocity and V_{trans} is the velocity of the cross flow, is expected to be approximately 0.5 [8]. Case C, is similar to Case A, except the cross flow is expected to be very weak resulting in a velocity ratio of R = 50. Finally, Case B represents a unit cell near the spanwise edge of the lower plenum. In this region the unit cell would experience a low to medium cross flow velocity, between the extreme limits of Case A and Case C, past an inline tube bundle post configuration.

Attention has been given to scaling of the expected flow in each of the previously described unit cell configurations. For a detailed description of non-dimensionalization and scaling in fluid flows the reader is suggested to see [17]. Utilizing the previously designed flow motivation skid [16], the maximum achievable Reynolds number in a single experimental jet will be approximately 74,000, while the maximum achievable jet Reynolds number when all six jets are run at equal flow rates, is approximately 36,000. In order to motivate the cross flow, an axial fan capable of producing jet to cross flow velocity ratios of 0.5-5, typical of what is experienced in the lower plenum, is used. The specified axial fan, which can motivate nearly 15,000 cfm of air in the setup, yields a maximum Reynolds number based on the test section's hydraulic diameter of approximately $1.32 \cdot 10^6$. The maximum transverse Reynolds number achievable in the facility is about 100,000. Similarly, the maximum achievable post Reynolds number in the facility is approximately 140,000 with a vortex shedding frequency of 440 Hz. The maximum temperature difference in the unit cell experiment is the same as the maximum producible in the flow skid (i.e., $\Delta T = 100$ K).

Geometric scaling was selected to be similar to that of the MIR facility developed by INL which utilized a 6.55:1 scale model [3-11]. The scale model used at INL had a jet diameter of 22.10 mm (0.87 in), the present unit cell facility includes a scaling of 6.598:1 such that standard tubing sizes (0.875 in) could be used. Based on this same scaling, the post diameter was 31.75 mm (1.25 in) with a scaled plenum height of 217.4 mm (8.56 in). The width of the experimental test section was selected as 610 mm (24 in), or approximately 2.5 times the width of the hexagonal array.

After addressing desired flow requirements for scaling of the experiment, concern was given to what temperature and velocity measurements were both possible and desired. PIV measurements were determined to be a sufficient method of capturing the velocity fields. Olive oil was chosen as the seeder particle for this application. The TSI Six-Jet Atomizer 9306 was chosen as the dispersion method for the seeding material and is capable of injecting particles with a flow rate of 2.4 L/hr per jet. Olive oil is dispersed at a particle size range of 0.1 to 2.0 μm with a 0.3 μm mean diameter, and a concentration of 10^7 particles/cm^3. The insertion point in the wind tunnel, where the atomizer will be connected, is located upstream of the fan. To ensure a mass balance in the system, an exit will also be cut out of the ducting which will then reconnect to the flow motivation skid. It was determined that to have 20% by volume of the wind tunnel be olive oil seeder particles, the atomizer will need to run for just under 2 hours. This is an over estimate of the amount of seeder particle needed in the system, and the true amount required will need to be determined empirically. With the mean diameter of 0.3 μm, the olive oil seeder particles will stay buoyant in the closed loop wind tunnel even without the cross flow being generated. This implies that the seeder injection will only need to be performed once over an extended period of time.

Creating temperature maps of the flow is a significant challenge. The thermal mixing effects for this scenario will primarily be quantified from the temperature fluctuations at the surface and through the support cylinders. In order to measure the attenuation of temperature fluctuations in the posts, four thermocouples were placed in each of the six outer posts, and aligned radially towards the center post. Additionally, four thermocouples were placed in the center post which has been designed to rotate 180° to gather temperature data at multiple radial and azimuthal locations.

The experimental test section shown for the unit cell is shown in Figure 5. As shown, the experimental test section has six vertical jets, with custom built honeycomb flow conditioners positioned upstream of the jet. The six jets issue into a honeycomb array of support posts. Additionally, a conditioned crossflow is introduced upstream of the support posts which interacts and redirects the flow of the jets to be horizontal toward the outlet of the test section. In the following section each component of the custom built wind tunnel facility, which produces the cross flow, is discussed in detail.

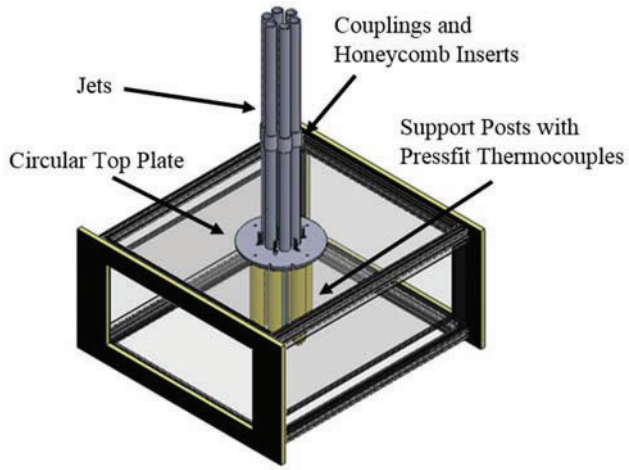

Figure 5 - Isometric View of the Test Section with Key Design Components Highlighted

4. DESIGN OF FACILITY

After appropriately identifying the functional requirements for the test section, and addressing design issues with the desired measurements, the next major concern was cross flow conditioning. In order to take consistent and meaningful velocity measurements that easily enable validation studies, it is ideal to have a uniform cross flow past the unit cell. In order to avoid seeing particles emptying into the room, a closed loop system was chosen. The closed loop system design consisted of several key components, including an axial fan, settling chamber, contraction nozzle, and diffuser as seen in Figure 6.

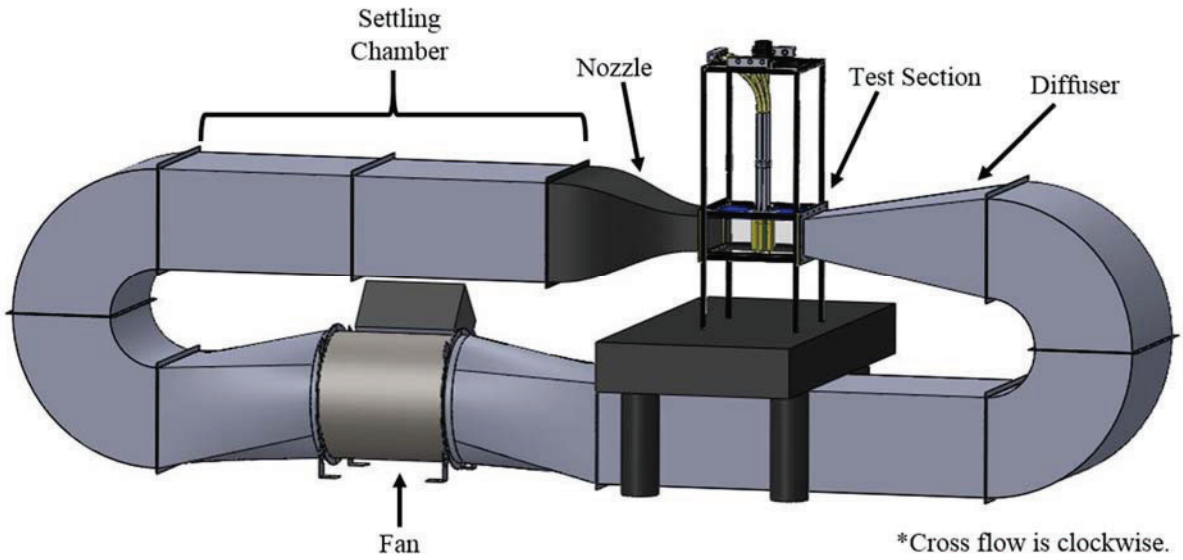

Figure 6: Cross Flow Wind Tunnel Design

In order to meet the desired cross flow Reynolds numbers and transverse velocity ratios presented in the scaling analysis, an axial fan was specified for flow motivation in the recirculating wind tunnel. As shown above in Figure 6, the fan sits on the ground upstream of and beneath the settling chamber. The settling chamber is required to straighten out the turbulent disruptions of the mean flow induced by the fan and 180˚ ducting elbow. Downstream of the settling chamber is the nozzle, which is built using standard wind tunnel design tools, establishes a uniform flow profile with minimal flow perturbations. The next component of the recirculating wind tunnel is the test section. The test section contains the hexagonal array of support posts as well as hexagon array of jets which enter orthogonally through the top plate. The diffuser is located downstream of the test section, and scales the cross sectional area of the test section back to that of the surrounding ducting, reducing mean velocity and pressure drop with it. All of these components' design parameters as well as their functionality are herein explained in greater detail.

From previous scaling studies, it was desired to have a minimum transverse velocity ratio of 0.5 between the cross flow velocity and the jet velocity. In order to create sufficient cross flow velocities to maintain a low transverse velocity ratio when all six jets are operating with a jet Reynolds numbers of 35,000, a crossflow flowrate of 11,000 cfm was necessary. Accordingly, after developing analytical models for the system pressure drop curves, the Greenheck mixed flow fan (model QEI-22-I-50) was selected. The QEI-22-I-50 provides a flow rate of 12,000 cfm overcoming up to 0.5 inH20 pressure drop with a maximum volumetric flow rate of 14,910 cfm. The fan itself has a diameter of 30.88 in requiring that custom round-to-square transitions were fabricated to mate the fan to the rectangular 3 ft x 2 ft ducting. The fan's gear box was also rotated to the 9 o'clock position to allow clearance for the ductwork overhead, as seen in Figure 6.

The effective length of the settling chamber was limited by the available lab space. The effective length is therefore 8 ft long. In this length, flow straightening devices were utilized to help straighten and allow for better control of the turbulent intensity distribution in the flow. Two aluminum hexagonal honeycomb inserts were utilized to aid in reducing large scale structures such as swirl from the flow as well as lateral mean velocity variations. A stainless steel wire mesh screen was incorporated to make the flow velocity more uniform. The design of the honeycomb and wire mesh was done in accordance with studies presented by Metha [18] and Scheiman [19]. The screen selected had a wire diameter of 0.054 in with a spacing of 3x3 wires per square in. The open area ratio for the screen was approximately 0.702 resulting in a pressure drop coefficient of 0.339 [20]. The screen was placed directly on the exit of the downstream honeycomb insert. Similar design was done for the honeycomb flow straighteners. Based on these sources, a honeycomb hydraulic diameter of 1 in was selected, with a total length of 6 in, or $L/D_{hyd} = 6$. The honeycomb inserts were placed at the entrance and exit of the settling chamber.

Following downstream of the settling chamber is the nozzle. The contraction nozzle, whose shape was determined following guidelines described by Metha [21], was designed to achieve a uniform cross flow by reducing both the mean and fluctuating velocity variations to a smaller fraction of the average velocity while simultaneously eliminating flow separation and reducing Moffatt eddies in the corners. The curve of the nozzle consists of a fifth order polynomial shown in Eq. (1). For the horizontal contraction dimensions, the inlet radius, H_i, was 18 in while the outlet radius, H_e, was 9 in. For the vertical dimensions of the contraction, the inlet radius was 12 in while the outlet radius was approximated as 4.25 in. The total length of the contraction, L, was 36 in. The nozzle design has a contraction ratio, defined as the ratio of inlet to outlet area, of 8.47. The nozzle which was constructed using 2 x 2 weave carbon fiber layups (from HEXCEL Composites [22]) is shown in Figure 6. The final nozzle design requires a 2 ft x 3 ft cross section for flow approaching the nozzle.

$$y(x) = H_i - \left(H_i - H_e\right)\left[6\left(\frac{x}{L}\right)^5 - 15\left(\frac{x}{L}\right)^4 + 10\left(\frac{x}{L}\right)^3\right] \tag{1}$$

The next portion downstream of the nozzle is the test section. Several design parameters were incorporated with the test section to allow for accurate and relevant velocity and temperature measurements to be found with the proper scaled design. First, a closer look at the test section is presented in Figure 5 and Figure 7. The first part of the test section are the jets which run vertically into the test section. Each of these jets contains two 12 in straight pipes with an inner diameter of 0.875 in, and are connected with a custom made coupling. Inside each of the couplings is a high temperature ceramic honeycomb insert for flow straightening and improved uniform turbulence statistics. These honeycomb flow straighteners are composed of Somos ® NanoTool with a glass transition temperature of 192 ˚F and consist of $L/D_{hyd} = 20$. The jet array can be seen in Figure 8a while an individual honeycomb flow straightener can be viewed with a transparent version of its jet in Figure 8b.

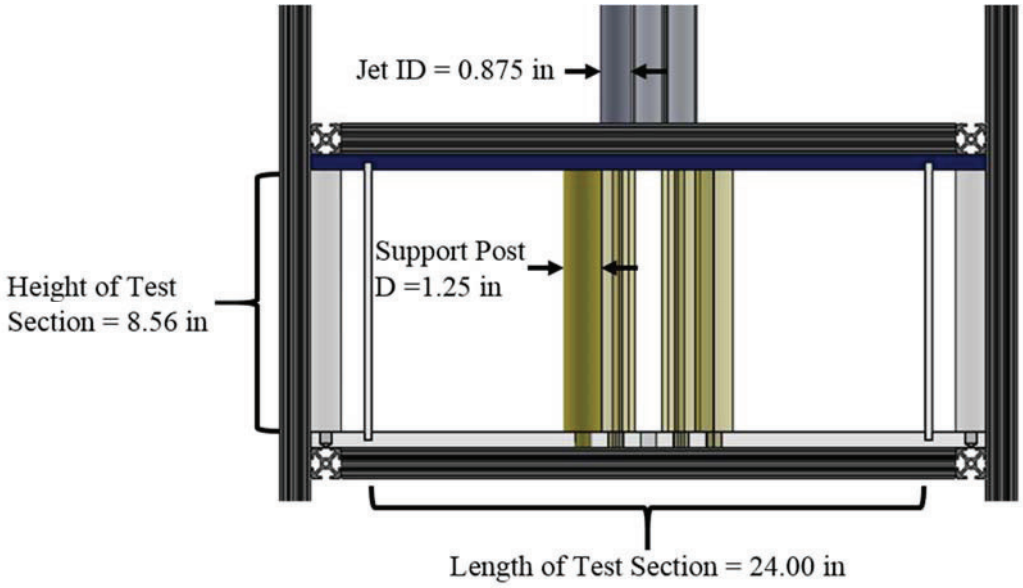

Figure 7: Front Face of Test Section with Notable Dimensions Included

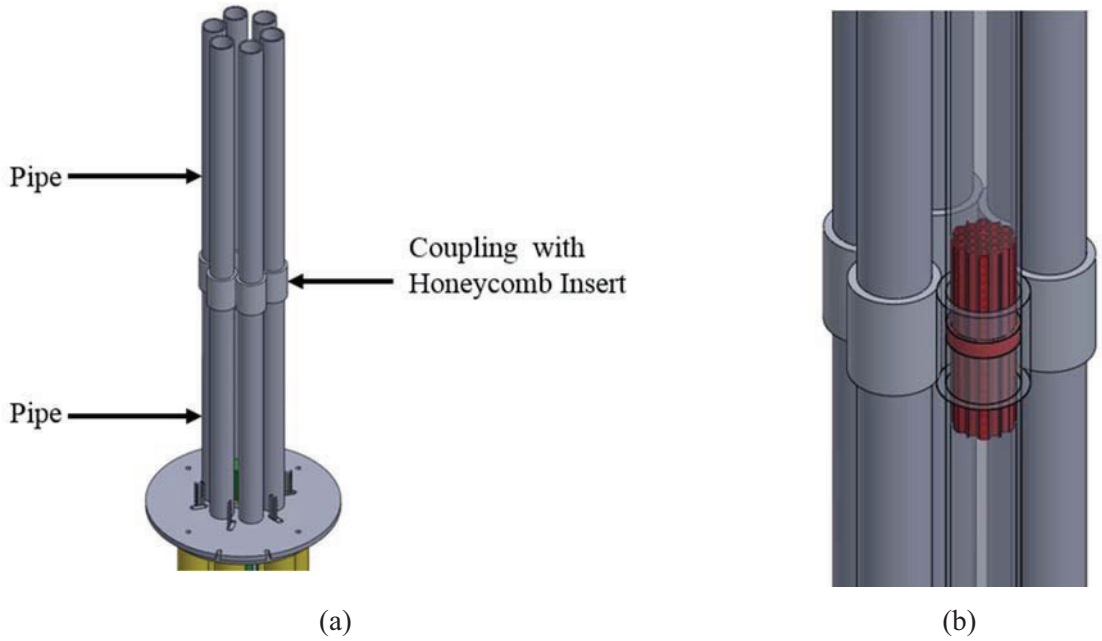

Figure 8: (a) Array of Six Jets Located Above Test Section (b) Transparent Jet Revealing Internal Honeycomb Insert

Also seen in Figure 5, is the circular aluminum top plate of the test section which holds the six hexagonal posts and the central support post. The top plate supports the jets, as well as aligns the outer support posts in the top wall of the test section. A more detailed view of the circular top plate with support posts, thermocouples, and jet inlets is shown in Figure 9. The aluminum circular plate locates each support post utilizing a four thermocouple press fit assembly (described later), with the exception of the rotating center post, which is secured with a press fit bushing. Additionally, the aluminum plate locates each jet in space. Finally, this aluminum plate was designed such that it can be rotated 30°, to accommodate flow across an inline tube bundle (case B in Figure 4) and a staggered tube bundle (cases A and C in Figure 4) . In order

to allow PIV measurements, the side walls and bottom plate were constructed from LEXAN®, a high temperature polycarbonate plastic that is optically transparent. Additionally, in order to reflect the laser sheet, which is inserted laterally through the sides into the test section, all posts were given a high accuracy mirror finish polish after being machined. The top wall was constructed from a high temperature, ultrahigh-molecular weight (UHMW) plastic.

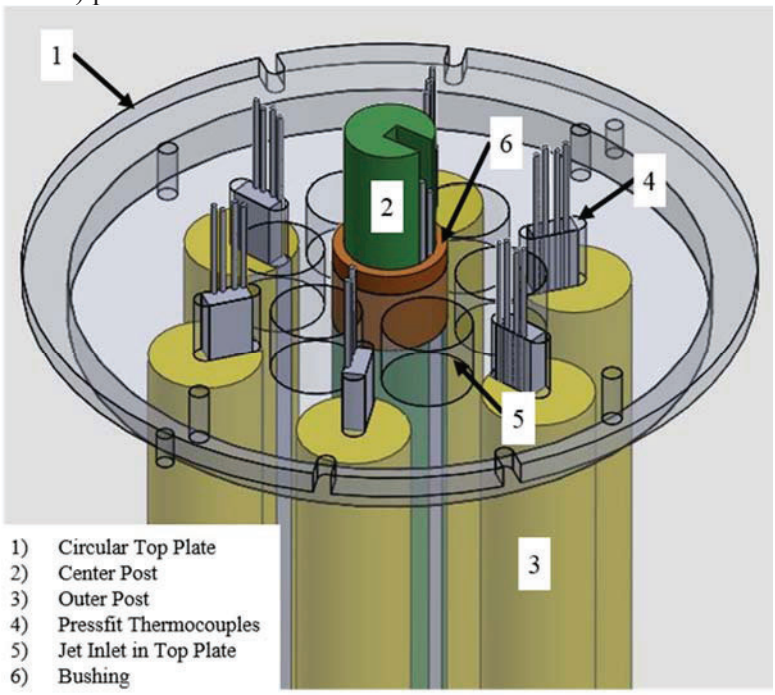

Figure 9: Transparent Circular Top Plate with Post Configuration

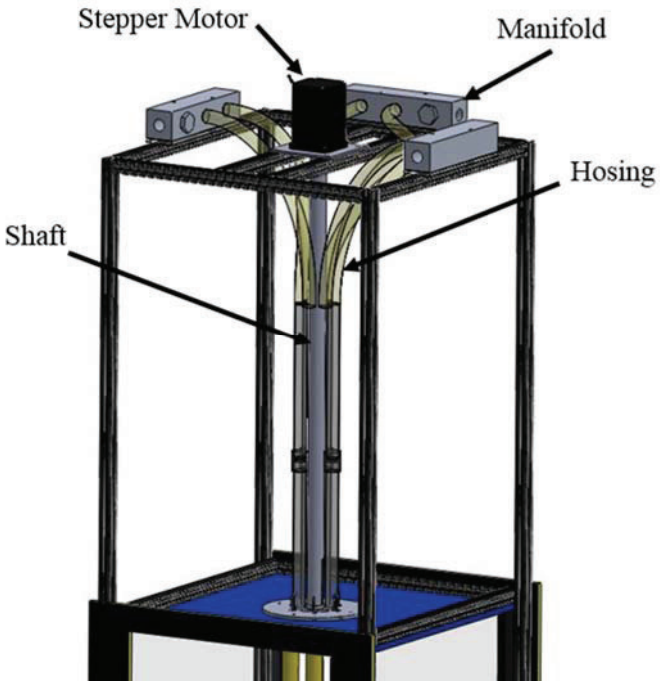

Figure 10: Stepper Motor Coupled to Center Post via a Shaft

In order to capture a radial map of the temperature in each post four thermocouples are inserted into each post from the top flat surface of the cylinder. The insertion depth, L, for two of the thermocouples is 2.16 in (L/H = 0.25), while the insertion depth for the other two thermocouples is 4.33 in (L/H = 0.5), where H is the height of the test section. These four thermocouples are also located at different radial positions within the cylinder, namely r/D =0.131 and 0.369 for the L/D = 0.25 thermocouples, and r/D=0.231 and 0.469 for the L/D = 0.5 thermocouples. In order to achieve accurate location of the thermocouples, a "press fit insert" was designed, to overcome machining limitations associated with large aspect ratio holes. Shown in Figure 11 is the press fit achieved with the insert and a transparent post for clarity. Similarly shown in Figure 9 is the thermocouple press fit which used to locate the posts in space as well as secure the thermocouples. In order to also capture an azimuthal map of temperature in the center post a stepper motor assembly was designed to automate rotation of the center post during tests. The stepper motor assembly is shown in Figure 10.

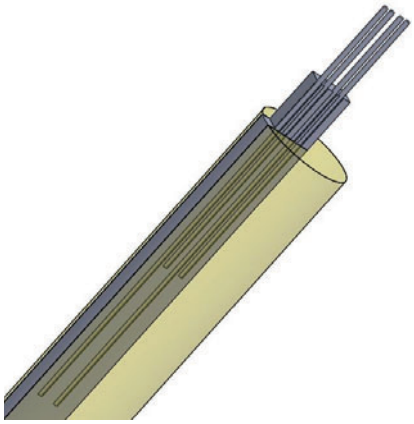

Figure 11: Transparent Post with Internal Thermocouple/Insert Assembly

Additionally, it should be noted that the manifolds in Figure 10 are used to connect the six jets to the previously designed flow motivation skid [16]. This allows for up to three unique jet temperatures to be independently controlled, as is required for Case A and C (Figure 4). Similarly, by utilizing just two manifolds it is possible to have only two unique temperatures so that Case B (Figure 4) can be studied.

The last component designed was the diffuser. The diffuser design process was much simpler than that for the nozzle design since no flow conditioning characteristics need to be considered downstream of the test section. Therefore, a simple linear expansion was utilized to scale the ducting from the 24 in x 8.56 in cross section of the test section to that of the 3 ft x 2 ft ducting. For proper mating and convenient dimensioning, the diffuser is also 4 ft in length. The diffuser and the remainder of the ducting in the close loop system, are all composed of stainless steel.

5. CONCLUSIONS

The proposed design for the Generation IV high temperature gas reactor causes concern regarding the thermal mixing taking place in the lower plenum. Idaho National Laboratory (INL) researchers [3-11] have performed numerous experimental studies in their matched index of refraction (MIR) facility aimed at characterizing the turbulence in the VHTR lower plenum, of which only incorporates isothermal flows. The scaled non isothermal unit cell facility design included in this study provides insight into the thermal mixing taking place in the lower plenum, particularly in thermal streaking in the structural support posts. The crossflow is herein simulated with the use of an axial fan, capable of 14,910 cfm of air in the setup, with a maximum Reynolds number based on the test section's hydraulic diameter of approximately $1.32 \cdot 10^6$. The jet flow is simulated by an array of six jets whose outlets are located above the unit cell. An individual jet is capable of a maximum Reynolds number of $7.4 \cdot 10^4$, while all six jets at equal flow rates are capable of

a maximum Reynolds number of $3.6 \cdot 10^4$. This provides for jet to cross flow velocity ratios of 0.5-5, which is characteristic of what is seen in the VHTR lower plenum. The maximum transverse Reynolds number, based on the transverse average velocity and jet diameter, is approximately $1.0 \cdot 10^5$. The maximum post Reynolds number is approximately $1.4 \cdot 10^5$. The maximum temperature difference in the unit cell experiment is ΔT=100°C, with a maximum operating temperature of 150°C, due to material restrictions. Various jet to cross flow ratios and temperature differences will be studied with the use of Particle Image Velocimetry instrumentation and embedded thermocouples in the posts, respectively. Tests will be conducted in the three notable post configurations as previously discussed. These experiments will offer insight into the thermal stresses that the structural support posts in the lower plenum of the VHTR are susceptible to for future work in material analysis of structural integrity in the VHTR core.

ACKNOWLEDGEMENTS

This research is being performed using funding received from the DOE Office of Nuclear Energy's Nuclear Energy University Programs. Additional thanks to the Swanson School of Engineering Office of Research, Swanson Center for Product Innovation and the University of Pittsburgh Formula SAE team for assistance in the labor intensive nozzle fabrication procedures The help from various undergraduate senior design teams is also acknowledged.

REFERENCES

1. Anderson, N., Hassan, Y. and Schultz, R. 2008. Analysis of the hot gas flow in the outlet plenum of the very high temperature reactor using coupled RELAP5-3D system code and CFD code. Nuclear Engineering and Design. 238(1), 274–279.
2. S. Mazumdar, D.T. Landfried, A. Jana, and M. Kimber, "Initial computation study of the thermal mixing in a VHTR lower plenum," *Proceedings of 15th International Topical Meeting on Nuclear Reactor Thermal Hydraulics (NURETH-15)*, Pisa, Italy, May12-17, 2013 (2013).
3. K. G. Condie, G. E. McCreery, H. M. McIllroy, and D. M. McEligot, "Development of an experiment for measuring flow phenomena occurring in a lower plenum for VHTR CFD Assessment," INL/EXT-05-00603, (2005).
4. H. M. McIllroy, D. M. McEligot, and R. J. Pink "Measurement of turbulent flow phenomena for the lower plenum of a prismatic gas-cooled reactor," *Nuclear Engineering and Design*, **240**(2), pp. 416-428 (2010).
5. D. P. Guillen, and H. M. McIllroy, "Preliminary study of turbulent flow in the lower plenum of a gas-cooled reactor," *Proceedings of 12th International Topical Meeting on Nuclear Reactor Thermal Hydraulics (NURETH-12)*, Pittsburgh, PA, USA, September 30-October 4, 2007 (2007).
6. D. P. Guillen, "Computational flow predictions for the lower plenum of a high-temperature, gas-cooled reactor," *Transactions of the American Nuclear Society*, **95**, pp. 827-828 (2006).
7. R. W. Johnson, "Modeling strategies for unsteady turbulent flows in the lower plenum of the VHTR," *Nuclear Engineering and Design*, **238**(3), pp. 482-491 (2007).
8. K. G. Condie, G. E. McCreery, H. M. McIllroy, and D. M. McEligot, "Development of an experiment for measuring flow phenomena occurring in a lower plenum for VHTR CFD Assessment," INL/EXT-05-00603, (2005).
9. D.M. McEligot and G. E. McCreery, "Scaling studies and conceptual experiment designs for NGNP CFD Assessment," lNEEL/EXT-04-02502, 30 November, 2004 (2004).
10. G.E. McCreery, and K. G. Condie, "Experimental Modeling of VHTR plenum flows during normal operation and pressurized conduction cooldown," INL/EXT-06-11760
11. H.M. McIlroy, D.M. McEligot, and R.J. Pink, "Measurement of turbulent Flow Phenomena for the Lower Plenum of a Prismatic Gas-Cooled Reactor," *Proceedings of 12th International Topical*

Meeting on Nuclear Reactor Thermal Hydraulics (NURETH-12), Pittsburgh, PA, USA, September 30-October 4, 2007 (2007).
12. B.L. Smith, J.J. Stepan, and D.M. McEligot, "Velocity and pressure measurements along a row of confined cylinders." *Journal of Fluids Engineering*, **119**, pp 1314-1327, 2007.
13. N. Amini and Y.A. Hassan, "Measurements of jet flow impinging into a channel contain a rod bundle using dynamic PIV," *International Journal of Heat and Mass Transfer*, **52**, pp. 5479-5495 (2009).
14. B. Wilson, J. Harris, B. Smith, and R. Spall, "Unsteady validation metrics for CFD in a cylinder array," *ASME 3rd Joint US-European Fluids Engineerign Summer Meeting*, pp. 2265-2278, 2010.
15. S.B. Rodriquez and M.S. El-Genk, "On Enhancing VHTR Lower Plenum Heat Transfer and Mixing via Swirling Jet," *Proceedings of 2010 International Congress on Advances in Nuclear power Plants (ICAPP'10)*, San Diego, California, USA, June 13-17, 2010 (2010).
16. D.T. Landfried, B. Goclano, and M. Kimber, "Design of a scaled non-isothermal experimental facility for studying the thermal hydraulics of the lower plenum of a prismatic VHTR," *Proceedings of the 15th International Topical Meeting on Nuclear Reactor Thermal Hydraulics (NURETH-15)*, Pisa, Italy, May12-17, 2013 (2013).
17. R. L. Panton, "Incompressible Flows," John Wiley and Sons, 2006.
18. R. D. Mehta, "Turbulent Boundary Layer Perturbed by Screen," *American Institute of Aeronautics and Astronautics Journal*, **23(**9), pp. 1335-1342 (1985).
19. J. Scheiman, "Comparison of Experimental and Theoretical Turbulence Reduction Characteristics for Screens, Honeycomb, and Honeycomb-Screen Combinations," *NASA Technical Paper*, (1958).
20. R.D. Metha, P. Bradshaw, "Design Rules for Small Low Speed Wind Tunnels," *Journal of Royal Aeronautical Society*, **73**, pp. 442-449 (1979).
21. J.H. Bell, and R.D. Mehta. "Contraction design for small low-speed wind tunnels," *NASA Contractor Report* NASA-CR-177488 (1988).
22. HEXCEL Composites, "HexWeb™ Honeycomb Attributes and Properties: A comprehensive guide to standard Hexcel honeycomb materials, configurations, and mechanical properties," (1999).